Lecture 11: Effective electrical tissue properties imaging

Habib Ammari

Department of Mathematics, ETH Zürich

Spectroscopic electrical tissue property imaging

- Diagnosis and staging of cancer disease.
- Help surgeons to make sure they removed everything unwanted around the margin of the cancer tumor.
- Perform biopsy in the operating room.

Spectroscopic electrical tissue property imaging

Electrical impedance system of electrodes:

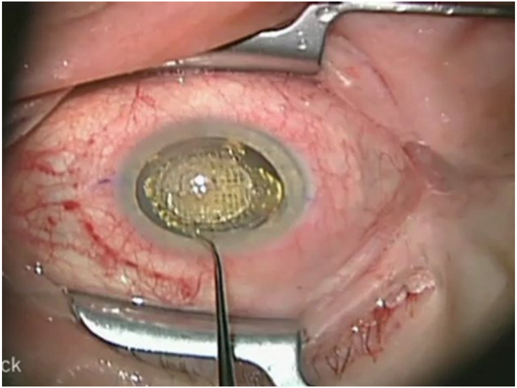

Spectroscopic electrical tissue property imaging

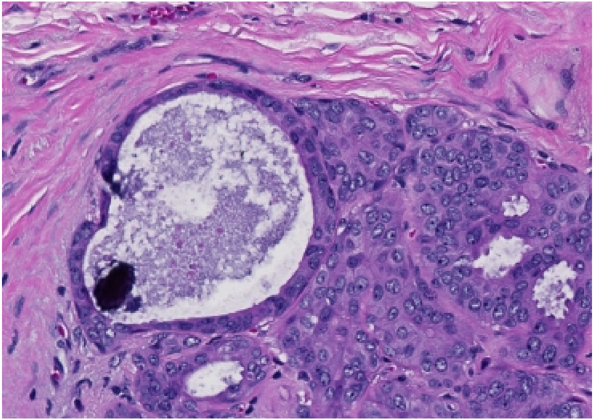

Spectroscopic electrical tissue property imaging

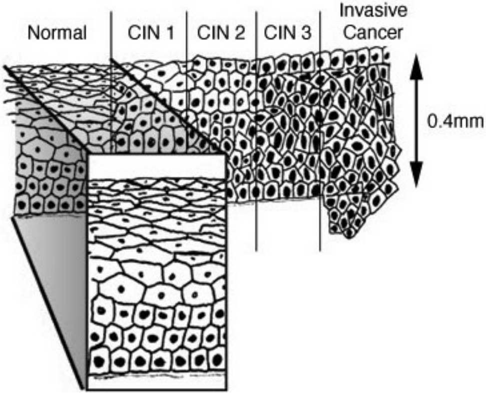

Spectroscopic electrical tissue property imaging

- Admittivities of biological tissues vary with the frequency $\omega \leq 10$ MHz of the applied sinusoidal current.
- Admittivities of biological tissues may be anisotropic at low frequencies, but they become isotropic as the frequency increases.
- Cell: homogeneous core covered by a thin membrane of contrasting electric conductivities and permittivities.
  - Intra and extra-cellular media: $k_0 := \sigma_0 + i\omega\varepsilon_0$ (conducting effect; transport of charges);
  - Membrane: $k_m := \sigma_m + i\omega\varepsilon_m$ with $\sigma_m/\sigma_0 \ll 1$ (capacitance effect; storage or charges or rotating molecular dipoles);
  - Thickness of the membrane $\ll$ typical size of the cell.

Spectroscopic electrical tissue property imaging

- Cell membrane phenomena:
  - Low frequencies: induced polarization effect due to the membrane.
  - High frequencies: induced polarization effect disappears.
- Electrical tissue property:
  - Pointwise at microscopic scale;
  - Effective at macroscopic scale: linear relationship between the ensemble mean current density and the ensemble mean electrical field;
  - Apparent: electrical tissue property of locally homogeneous and isotropic medium $=$ potential measured on the heterogeneous subject using the same applied current and arrangement of the electrodes.

Spectroscopic electrical tissue property imaging

- Spectral properties of the effective admittivity: super-resolution in electrical imaging of biological tissues.
- Classification of micro-structure organization using spectroscopic admittivity imaging.
- Distance on the effective admittivity spectra to statistically differentiate tissues with different microstructures.
- Measure of the admittivity anisotropy and its dependence on the frequency of applied current.
    - Anisotropic tissues: muscles and nerves.
    - Clinical application: neuromuscular diseases lead to a reduction in anisotropy for a range of frequencies; muscle fibers replaced by isotropic tissue.

Spectroscopic electrical tissue property imaging

- Tissue model:

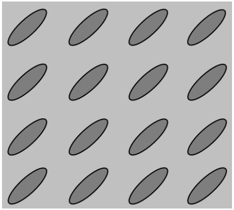

- δ: cell period;
- Ω_δ^+: extra-cellular medium;
- Ω_δ^-: intra-cellular medium;
- Γ_δ: cell membranes.
- Y: unit cell; $Y^\pm$: extra-cellular and intra-cellular (rescaled) media.

Spectroscopic electrical tissue property imaging

$$
\begin{cases}
-\nabla \cdot k_0 \nabla u_\delta^+ = 0 & \text{in } \Omega_\delta^+ \cup \Omega_\delta^-, \\
k_0 \dfrac{\partial u_\delta^+}{\partial \nu} = k_0 \dfrac{\partial u_\delta^-}{\partial \nu} & \text{on } \Gamma_\delta, \\
u_\delta^+ - u_\delta^- - \delta \, \xi \dfrac{\partial u_\delta^+}{\partial \nu} = 0 & \text{on } \Gamma_\delta, \\
\dfrac{\partial u_\delta^+}{\partial \nu} = g & \text{on } \partial\Omega.
\end{cases}
$$

- $u_\delta = u_\delta^\pm \text{ in } \Omega_\delta^\pm$;
- $\xi = \text{thickness} \times k_m / k_0$: effective thickness;
- g: electric field applied at $\partial\Omega$ of frequency ω ($\int_{\partial\Omega} g d\sigma = 0$).

Spectroscopic electrical tissue property imaging

- Homogenized problem:

$$\begin{cases} -\nabla \cdot K^* \nabla u_0(x) = 0 & \text{in } \Omega, \\ \dfrac{\partial u_0}{\partial \nu} = g & \text{on } \partial\Omega, \end{cases}$$

- Effective admittivity:

$$K^*_{i,j} = k_0 \left(\delta_{ij} + \int_Y \nabla w_i \cdot e_j \right),$$

Spectroscopic electrical tissue property imaging

- Cell problems ($i = 1, \ldots, d$; d: space dimension):

$$\begin{cases} -\nabla \cdot k_0 \nabla (w_i^+(y) + y_i) = 0 & \text{in } Y^+, \\ -\nabla \cdot k_0 \nabla (w_i^-(y) + y_i) = 0 & \text{in } Y^-, \\ k_0 \frac{\partial}{\partial \nu}(w_i^+(y) + y_i) = k_0 \frac{\partial}{\partial \nu}(w_i^-(y) + y_i) & \text{on } \Gamma, \\ w_i^+ - w_i^- - \xi \frac{\partial}{\partial \nu}(w_i^+(y) + y_i) = 0 & \text{on } \Gamma, \\ y \longmapsto w_i(y) \ Y\text{-periodic}. \end{cases}$$

- u_δ two-scale converges to u_0.
- ∇u_δ two-scale converges to $\nabla u_0 + \chi^+ \nabla_y u_1^+ + \chi^- \nabla_y u_1^-$.
- $\chi^\pm$: characteristic function of $Y^\pm$.
- Corrector:

$$\forall (x, y) \in \Omega \times Y, \ \ u_1(x, y) = \sum_{i=1}^{2} \frac{\partial u_0}{\partial x_i}(x) w_i(y).$$

Spectroscopic electrical tissue property imaging

- Spectroscopic imaging: $\omega \mapsto K^*(\omega)$;
- $K^*_{i,j}(\omega) = k_0 \left(\delta_{ij} + \int_Y \nabla w_i(\omega) \cdot e_j \right)$;
- Correctors:

$$\begin{cases} -\nabla \cdot k_0 \nabla (w_i^+(y) + y_i) = 0 & \text{in } Y^+, \\ -\nabla \cdot k_0 \nabla (w_i^-(y) + y_i) = 0 & \text{in } Y^-, \\ k_0 \dfrac{\partial}{\partial \nu}(w_i^+(y) + y_i) = k_0 \dfrac{\partial}{\partial \nu}(w_i^-(y) + y_i) & \text{on } \Gamma, \\ w_i^+ - w_i^- - \xi(\omega) \dfrac{\partial}{\partial \nu}(w_i^+(y) + y_i) = 0 & \text{on } \Gamma, \\ y \longmapsto w_i(y) \ Y\text{-periodic.} \end{cases}$$

Spectroscopic electrical tissue property imaging

The effective admittivity of a periodic dilute suspension:

$$K^* = k_0 \left(I + f M \left(I - \frac{f}{2} M \right)^{-1} \right) + o(f^2),$$

- $f = |Y^-| = \rho^2$: volume fraction;
- M: membrane polarization tensor

$$M = \left(m_{ij} = \beta k_0 \int_{\rho^{-1}\Gamma} \nu_j \psi_i^*(y) ds(y) \right)_{(i,j) \in [|1,2|]^2},$$

- $\psi_i^* = -\left(I + \beta k_0 L_{\rho^{-1}\Gamma}\right)^{-1} [\nu_i]$.
- $L_\Gamma[\varphi](x) = \dfrac{1}{2\pi} \mathrm{p.v.} \displaystyle\int_\Gamma \frac{\partial^2 \ln |x-y|}{\partial \nu(x) \partial \nu(y)} \varphi(y) ds(y), \quad x \in \Gamma.$

Spectroscopic electrical tissue property imaging

Maxwell-Wagner-Fricke Formula:

- Case of concentric circular-shaped cells.
- For $(i, j) \in [|1, 2|]^2$:

$$m_{i,j} = -\delta_{ij} \frac{\beta k_0 \pi r_0}{1 + \dfrac{\beta k_0}{2 r_0}}.$$

- $\Im M$ attains one maximum with respect to ω at $1/\tau$:

$$\Im m_{i,j} = \delta_{ij} \frac{\pi r_0 \delta \omega (\varepsilon_m \sigma_0 - \varepsilon_0 \sigma_m)}{(\sigma_m + \frac{\eta \sigma_0}{2 r_0})^2 + \omega^2 (\varepsilon_m + \frac{\eta \varepsilon_0}{2 r_0})^2}.$$

- η: membrane thickness.
- τ: relaxation time (in the β-dispersion region).

Spectroscopic electrical tissue property imaging

- Properties of the membrane polarization tensor:
  - M: symmetric;
  - M: invariant by translation;
  - $M(sC, \xi) = s^2 M(C, \frac{\xi}{s})$ for any scaling parameter $s > 0$.
  - $M(\mathcal{R}C, \xi) = \mathcal{R} M(C, \xi) \mathcal{R}^t$ for any rotation $\mathcal{R}$.
  - $\Im M$: positive and its eigenvalues have one maximum with respect to ω.
- Relaxation times for the arbitrary-shaped cells:

$$\frac{1}{\tau_i} := \arg \max_{\omega} \lambda_i(\omega),$$

$\lambda_1 \geq \lambda_2$: eigenvalues of $\Im M$.

- $(\tau_i)_{i=1,2}$: invariant by translation, rotation and scaling.

Spectroscopic electrical tissue property imaging

Shape of the cell and relaxation times: circle, an ellipse and a very elongated ellipse

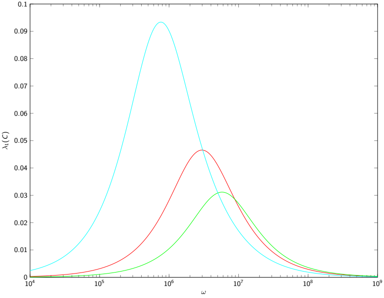

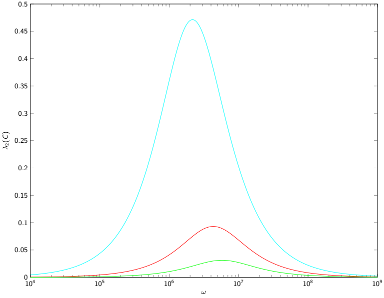

Spectroscopic electrical tissue property imaging

Frequency dependence of the eigenvalues of the membrane polarization tensors for the 3 different shapes of cell: circle, an ellipse and a very elongated ellipse with the same volume

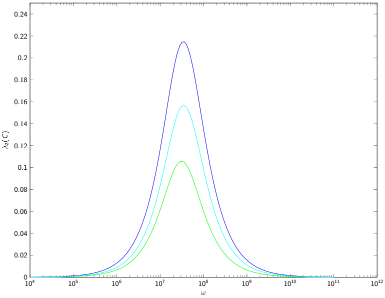

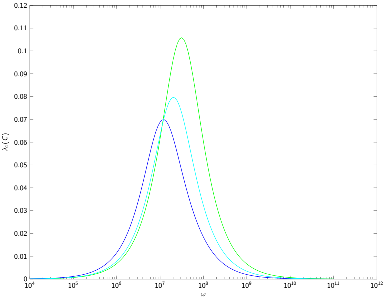

Spectroscopic electrical tissue property imaging

- Measure of the anisotropy:

$$\omega \mapsto \frac{\lambda_1(\omega)}{\lambda_2(\omega)}$$

- $\lambda_1 \leq \lambda_2$: eigenvalues of $\Im M(\omega)$.
- Large ω:

$$\frac{\lambda_1(\omega)}{\lambda_2(\omega)} = 1 + (l_1 - l_2)\frac{2\eta\sigma_m\rho}{(\sigma_m^2 + \omega^2\varepsilon_m^2)|\Gamma|} + O(\eta^2),$$

η: membrane thickness; $l_1 \leq l_2$: eigenvalues of $\int_{\rho^{-1}\Gamma} n\mathcal{L}_{\rho^{-1}\Gamma}[n]ds$.

- Anisotropic information not captured:

$$\omega \gg \frac{1}{\varepsilon_m}((l_1 - l_2)\frac{2\eta\sigma_m\rho}{|\Gamma|} - \sigma_m^2)^{1/2}.$$

Spectroscopic electrical tissue property imaging

- Electrolocation for weakly electric fish:
  - Electric organ: generate a stable, high-frequency, weak electric field.
  - Electroreceptors: measure the transdermal potential modulations caused by a nearby target.
  - Nervous system: locate the target, perceive its shape, determine its physical nature.

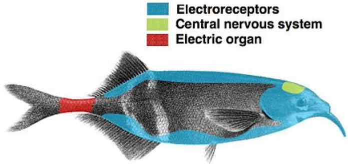

Spectroscopic electrical tissue property imaging

Mechanism for mimicking shape perception:

- Form an image from the perturbations of the field due to targets.
- Identify and classify the target, knowing by advance that it belongs to a learned dictionary of shapes.
  - Extract the features from the data.
  - Construct invariants with respect to rigid transformations and scaling.
  - Compare the invariants with precomputed ones for the dictionary.
- Biological targets: frequency dependent electromagnetic properties (capacitive effect generated by the cell membrane structure).
- Spectroscopic measurements of the target's polarization tensor.

Spectroscopic electrical tissue property imaging

- Wave-type electric signal: $f(x,t) = f(x)\sum_n a_n e^{in\omega_0 t}$; ω_0: fundamental frequency.

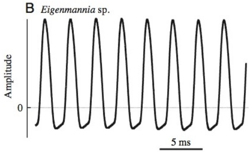

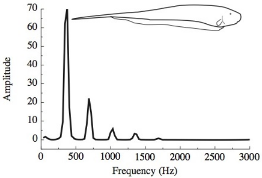

- Skin: very thin ($\delta \sim 100\mu$m) and highly resistive ($\sigma_s/\sigma_0 \sim 10^{-2}$); $\sigma_b/\sigma_0 \sim 10^2$ (highly conductive).

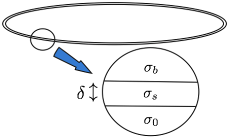

Spectroscopic electrical tissue property imaging

- Target $D = z + \delta' B$; z: location; δ': characteristic size of the target; $k(\omega) = (\sigma(\omega) + i\omega\varepsilon(\omega))/\sigma_0$; k, σ, and ε: the admittivity, the conductivity, and the permittivity of the target; $\omega_n = n\omega_0$: the probing frequency.
- u_n : the electric potential field generated by the fish:

$$\begin{cases} \Delta u_n = f, & x \in \Omega, \\ \nabla \cdot (1 + (k(\omega_n) - 1)\chi(D))\nabla u_n = 0, & x \in \mathbb{R}^2 \setminus \overline{\Omega}, \\ \left.\dfrac{\partial u_n}{\partial \nu}\right|_{-} = 0, \quad [u_n] = \xi \left.\dfrac{\partial u_n}{\partial \nu}\right|_{+} & x \in \partial\Omega, \\ |u_n(x)| = O(|x|^{-1}), \quad |x| \to \infty. \end{cases}$$

- $\xi := \delta\sigma_0/\sigma_s$ effective thickness.
- $\lambda(\omega_n) = (k(\omega_n) + 1)/(2(k(\omega_n) - 1))$.

Spectroscopic electrical tissue property imaging

- Dipole approximation: $u_n(x) - U(x) \simeq \mathbf{p} \cdot \nabla G(x-z)$.
  - G: Green's function associated to Robin boundary conditions.
  - Dipole moment $\mathbf{p} = - \underbrace{M(\lambda(\omega_n), D)}_{\text{Polarization tensor}} \nabla U(z)$.
  - Neumann-Poincaré operator:
    $$\mathcal{K}_D^*[\varphi](x) = \frac{1}{2\pi} \int_{\partial D} \frac{\langle x-y, \nu_x \rangle}{|x-y|^2} \varphi(y)\, ds(y) \,, \quad x \in \partial D.$$
  - $M(\lambda(\omega_n), D) = \displaystyle\int_{\partial D} x(\lambda(\omega_n) I - \mathcal{K}_D^*)^{-1}[\nu](x)\, ds(x)$.

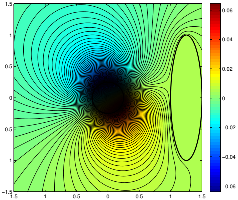

Spectroscopic electrical tissue property imaging

- Space-frequency response matrix: $(V_{sr}^n)_{rn}$

$$V_{sr}^n = \left(\frac{\partial u_n}{\partial \nu}(x_r)\Big|_+ - \frac{\partial U}{\partial \nu}(x_r)\Big|_+ \right),$$

  x_s: position of the electric organ; (x_r): receptors on the skin of the fish.
- Space-frequency location search algorithm.
- Movement: fish takes measurement at different positions around the target; use of only one frequency.

Spectroscopic electrical tissue property imaging

- Dipole approximation:

$$V_{sr}^n \simeq -\nabla U(z) \cdot \overbrace{M(\lambda(\omega_n), D)}^{\propto I} \cdot \left(\nabla \frac{\partial G}{\partial \nu_x}(x_r - z) \right);$$

- z^S in the search domain; $g(z^S)$ given by

$$\left(\nabla U(z^S) \cdot \nabla \left(\frac{\partial G}{\partial \nu_x} \right) (x_1 - z^S), \ldots, \nabla U(z') \cdot \nabla \left(\frac{\partial G}{\partial \nu_x} \right) (x_L - z^S) \right)^T;$$

- Subspace imaging functional:

$$\mathcal{I}(z^S) := \frac{1}{|(I-P)g(z^S)|};$$

P: orthogonal projection onto the first singular vector of $(V_{sr}^n)_{rn}$;

- $\mathcal{I}(z^S)$: large peak at $z^S = z$.

Spectroscopic electrical tissue property imaging

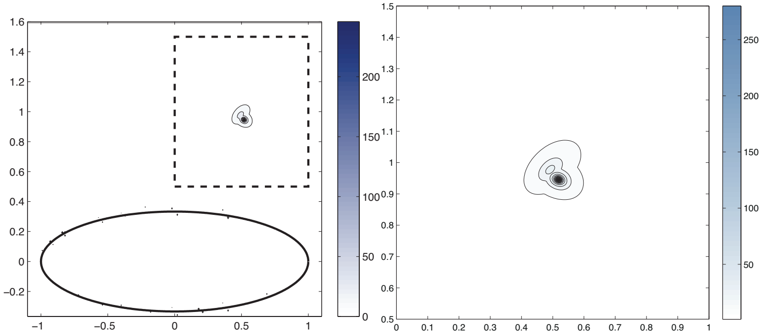

Number of frequencies: 10; number of receptors: 64.

- σ, ε: determined by minimizing a quadratic misfit functional.

Spectroscopic electrical tissue property imaging

- Multi-frequency approach: $\omega \mapsto M(\lambda(\omega), D)$.
  - Invariance with respect to translation, rotation, and scaling.
  - $\tau_j(\omega)$: eigenvalues of $\Im m\, M(\lambda(\omega), D)$; ω_∞: highest probing frequency. Plot
  $$\omega \mapsto \frac{\tau_j(\omega)}{\tau_j(\omega_\infty)},$$
  for $j = 1, \ldots, d$.

Spectroscopic electrical tissue property imaging

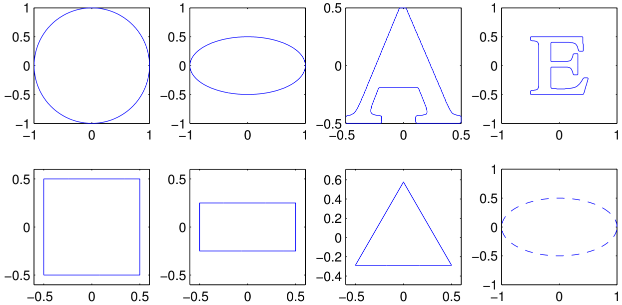

Spectroscopic electrical tissue property imaging

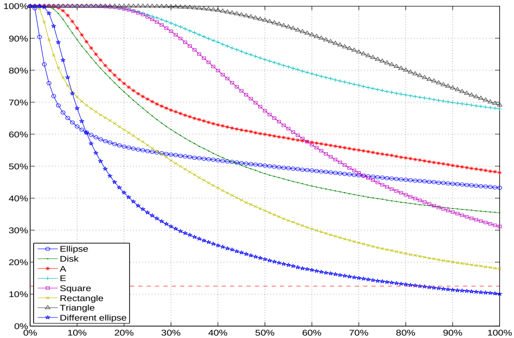

Probability of detection in terms of the noise level. Stability of classification based on differences between ratios of eigenvalues of $\Im m\, M(\lambda(\omega), D)$.

Spectroscopic electrical tissue property imaging

- Governing equation for pulsed-type imaging:

$$\begin{cases} \nabla \cdot (\sigma(x) + \varepsilon(x)\partial_t)\nabla u(t,x) = h(t)f(x) \;\; \text{in } \mathbb{R}^+ \times \mathbb{R}^2, \;\; , \\ |u(t,x)| = O(|x|^{1-d}) \;\; \text{as } |x| \to +\infty, t \in \mathbb{R}_+ \;\; , \\ u(0,x) = 0 \;\; \text{in } \mathbb{R}^2 \; . \end{cases}$$

- Pulse h: band pass filter ($\widehat{h}(0) = 0$); h_j: dyadic dilation of h:

$$h_j(t) = 2^{j/2} h(2^j t) \quad \text{and} \quad \widehat{h}_j(\omega) = 2^{-j/2} \widehat{h}(2^{-j}\omega).$$

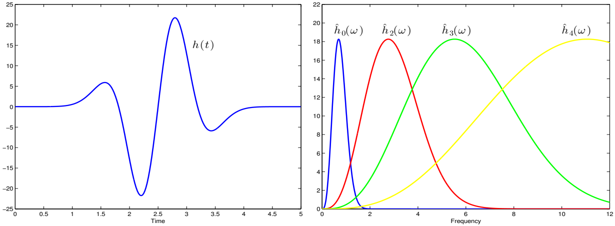

Spectroscopic electrical tissue property imaging

- Multi-scale shape descriptors.

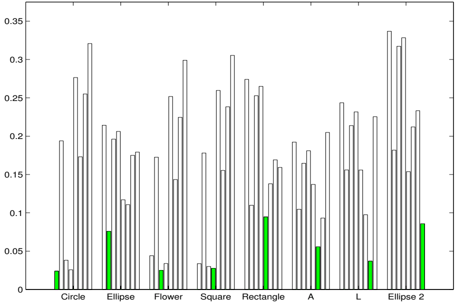

Results of identification with two scales 100% noise in a limited view configuration (aperture $= \pi/16$).